molecular pharmaceutics

ARTICLE

pubs.acs.org/molecularpharmaceutics

Differential Expression of the 18 kDa Translocator Protein (TSPO) by Neoplastic and Inflammatory Cells in Mouse Tumors of Breast Cancer

Jinzi Zheng,[†] Raphaël Boisgard,[†] Karine Siquier-Pernet,[†] Didier Decaudin,[‡] Frédéric Dollé,[§] and Bertrand Tavitian*[,†]

[†]Laboratoire d'Imagerie Moléculaire Expérimentale, Université Paris Sud, INSERM Unit 1023, 4 Place du Général Leclerc, F-91400 Orsay, France

[‡]Laboratory of Preclinical Investigation, Institut Curie, 26 rue d'Ulm, F-75248 Paris, France

[§]Institut d'Imagerie BioMédicale, Service Hospitalier Frédéric Joliot, Commissariat a l'Énergie Atomique, 4 Place du Général Leclerc, F-91400, France

ABSTRACT: Tumor-associated inflammation has been linked to angiogenesis, metastasis and poor prognosis. The 18 kDa translocator protein (TSPO), also known as the peripheral benzodiazepine receptor (PBR), is expressed in activated immune cells such as macrophages, but also in a number of cancer cell lines such as those of breast cancer. There is an increasing clinical interest in TSPO expression as it has been proposed as a poor prognostic factor for survival in lymph-node negative breast cancer patients. This study aims to assess of the presence of neoplastic cell-associated TSPO and tumor macrophage-associated TSPO in mouse xenografts generated from the MDA-MB-231 and the MCF-7 breast cancer cell lines, as well as 25 different breast tumors originally derived from patient-tissue but propagated in mice using two antibodies, each specific to either the human or the murine form of TSPO. Autoradiography with the TSPO ligand [^{18}F]DPA-714 and immunohistochemistry were also performed on the excised tumor tissues from the MDA-MB-231, MCF-7 and one of the patient-derived xenografts (HBCx-12B). High TSPO expression (either cancer or stromal cell-associated, or both) was measured in 20/25 (80%) of the patient-derived breast cancer xenografts. [^{18}F]DPA-714 showed displaceable binding to both the human and murine TSPO on tumor tissue sections. Immunohistochemistry demonstrated that a significant portion of the tumor stromal TSPO expression colocalized with F4/80 positive macrophages cells. This study constitutes a first report of the tumor TSPO expression by mixed cell populations, and it may have important implications for cancer biology as well as for the development of imaging and therapeutic ligands targeted to TSPO.

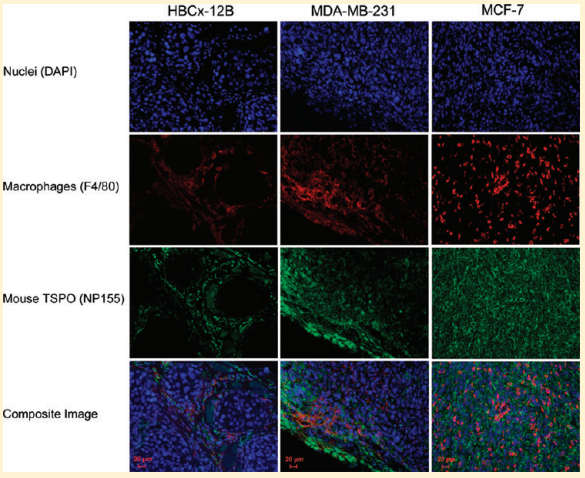

KEYWORDS: 18 kDa translocator protein (TSPO), peripheral benzodiazepine receptor (PBR), breast cancer, tumor-associated macrophages (TAM), DPA-714, positron emission tomography (PET)

INTRODUCTION

Breast cancer is the most common form of cancer in women. In the United States alone, 192 600 cases (27% of all cancer cases) were estimated in 2009.[1] Ongoing efforts in breast cancer research have led to earlier diagnosis and better targeted therapies which resulted in significantly lower mortality rates as well as improved quality of life for patients. However, breast cancer still remains the second leading cause of cancer-related deaths in women (15% of all cancer deaths in the United States in 2009[1]). There is, therefore, an ongoing need for accelerated development of more effective diagnostic and therapeutic strategies.

In recent years, much evidence has confirmed that the tumor microenvironment plays an important role in both disease progression and response to therapy.[2−7] Tumors are not exclusively composed of cancer cells; they are complex tissues in which cancer cells have recruited the surrounding nonmalignant cells (i.e., endothelial cells, immune cells and fibroblasts) to actively collaborate in their neoplastic activity.[3] It is therefore important to gain further understanding of the tumor microenvironment and its interplay with the neoplastic cells during disease progression so that improved therapeutic strategies can be developed to successfully control and ultimately cure cancer.

The 18 kDa translocator protein TSPO, also known as the peripheral benzodiazepine receptor (PBR), has been reported to be overexpressed in a number of cancer cell lines including breast, colorectal, prostate, ovarian, glioma, and hepatocarcinoma and has shown its involvement in the modulation of cell proliferation and tumorigenesis.[8] A previous publication has investigated the expression of TSPO in a panel of 9 breast cancer cell lines and has

Received: December 15, 2010
Accepted: March 21, 2011
Revised: February 22, 2011
Published: March 21, 2011

found that increased TSPO expression correlated with increased aggressive cancer cell phenotype.[9] Clinically, TSPO expression has been reported to be a potential poor prognostic factor for survival in lymph-node negative breast cancer patients.[10]

On the other hand, high expression of TSPO has been reported in immune cells such as macrophages and monocytes,[11−13] and TSPO is already a well-characterized marker of neuroinflammation.[13−15] Tumor-associated inflammation has been linked to angiogenesis, metastatic potential[2,7,16−19] and ultimately poor prognosis in patients.[20] Specifically, Lin et al.[18] demonstrated, in a transgenic mouse model of breast cancer (Polyoma Middle T oncoprotein, PyMT-induced mammary tumors), that tumor-associated macrophages (TAMs) are actively involved in triggering the angiogenic switch which is essential for tumor progression.[21] In addition, TAMs also play a role in the maintenance and remodeling of the established vessels network in malignant tumors.[22] More recently, DeNardo et al. reported on the ability of CD4+ T cells to regulate pulmonary metastasis through enhancement of protumor properties of macrophages in the same mouse mammary tumor virus (MMTV)-PyMT mouse model of mammary carcinoma.[17] A clinical study also correlated elevated levels of biomarkers for inflammation, such as the serum amyloid A (SAA) and the C-reactive protein (CRP), to reduced survival in breast cancer patients.[20] Recent evidence suggests that there is even a possibility that metastatic cancers can arise from cells of the myeloid/macrophage lineage independent of their primary tissue origin.[23]

To date, no study has yet employed cell line derived preclinical tumor models to validate the *in vitro* results nor assessed the TSPO expression in patient tumor derived xenograft models. It is important that this validation in preclinical models is performed before any conclusions from cell line based investigations are used to support clinical data. Furthermore, no investigation has searched for expression of TSPO in cell populations that make up the tumor stroma (i.e., in the tumor-associated macrophage cells), nor quantified its relative contribution to the total TSPO density in a tumor. As a result, there is no knowledge on the potential role of macrophage-associated TSPO in the progression and metastasis of breast cancers. Improved understanding of the expression of TSPO in different cell types in *in vivo* models of disease will also further enable more effective employment of anti-TSPO ligands as therapeutic vectors[24] or as targeting moieties for drug delivery systems.[25−31] A recent study[29] has demonstrated that, *in vitro*, a synergistic cytotoxic effect against LN 18 human glioblastoma cells was measured by incorporating the TSPO ligand CB86 onto the surface of paclitaxel-loaded polymer micelles. Therefore, in tumors with significant expression of TSPO on both malignant cancer cells and metastasis-promoting TAMs, TSPO-targeting drug delivery vehicles would have the potential to achieve an even greater therapeutic effect.

The aim of this study is to distinguish the presence of neoplastic cell-associated TSPO from that of tumor macrophage-associated TSPO in mouse xenografts of human breast cancer derived from two cell lines (MDA-MB-231 which has been reported to have high TSPO expression and MCF-7 which has been reported to have extremely low TSPO expression) and from 25 patient tumor tissues.[32] The successful differentiation of the cancer and stromal cell-associated TSPO will allow for multiparametric and potentially improved prognostic analysis, as well as lead to the development of more specific imaging and therapeutic vectors targeted to the TSPO overexpressing cell population of choice.

EXPERIMENTAL SECTION

Radiochemicals and Chemicals. *N*,*N*-Diethyl-2-(2-(4-(2-fluoroethoxy)phenyl)-5,7-dimethylpyrazolo[1,5-*a*]pyrimidin-3-yl)acetamide (DPA-714) was labeled with fluorine-18 (half-life 109.8 min) at its 2-fluoroethyl moiety using a tosyloxy-for-fluorine nucleophilic aliphatic substitution according to slight modifications of procedures already reported.[33] This simple one-step process has been automated on our Zymate-XP robotic system[34] and then implemented on a commercially available GE TRACERLab FX-FN synthesizer. The process involves (A) reaction of K[^{18}F]F-Kryptofix222 with the tosyloxy precursor (4.5−5.0 mg, 8.2−9.1 μmol) at 165 °C for 5 min in DMSO (0.6 mL) followed by (B) C-18 PrepSep cartridge prepurification and finally (C) semipreparative HPLC purification on a Waters X-Terra RP18. Final formulation of [^{18}F]DPA-714 as an iv injectable solution (physiological saline containing less than 10% of ethanol) was performed using a homemade SepPakPlus C18 device. Typically, 5.6−7.4 GBq of [^{18}F]DPA-714 (>95% chemically and radiochemically pure) was routinely obtained with specific radioactivities ranging from 37 to 111 GBq/mmol within 85−90 min (HPLC purification and SepPak-based formulation included), starting from a 37 GBq [^{18}F]fluoride batch (overall non-decay-corrected and isolated radiochemical yield: 15 to 20%). Stock solutions of PK11195 or DPA-714 to be used in autoradiography were prepared by dissolving 2 to 3 mg of (*R*,*S*)-PK 11195 (respectively DPA-714) in 200 μL of DMSO (at room temperature) and were used within one hour.

Animal Models. All experiments were performed under an animal use and care protocol approved by the animal ethics committee, and they were conducted in accordance with the European Union regulations on animal research. MDA-MB-231 and MCF-7 human breast cancer cell lines were purchased from ATCC-LGC Standards and maintained in culture using the Dulbecco's modified Eagle's medium (DMEM, purchased from Sigma-Aldrich) containing 10% fetal bovine serum (FBS) and 1% antibiotics. Once the cells reached >90% confluency, 5×10^6 cells were subcutaneously injected (in 1:1 volume ratio of DMEM with FBS and antibiotic supplement and Matrigel (BD Biosciences) into the flanks of female nude NMRI mice (purchased from Elevage Janvier, France). The mice inoculated with MCF-7 cells were implanted with a 17β-estradiol pellet (0.72 mg/pellet, 60-day release, purchased from Innovative Research of America, Sarasota, FL, USA) under their dorsal skin 24 h before. A third group of mice were surgically implanted with a small piece of a freshly resected HBCx-12B tumor obtained from a donor mouse bearing a patient-derived tumor (kindly provided by Institut Curie, Paris, France). A detailed description of the origin and tumor characteristics of HBCx-12B, as well as the other 24 patient-derived xenograft samples, was previously reported by Marangoni et al.[32] The PyMT model used as the murine control for TSPO expression in the Western blot studies was established on female FVB/NRj mice (purchased from Elevage Janvier, France) by subcutaneously implanting a small piece of a freshly resected MMTV-PyMT tumor from the mammary gland of the transgenic mouse.

Western Blot. Proteins were extracted from MDA-MB-231 and MCF-7 cultured cell suspensions, as well as from MDA-MB-231, MCF-7, HBCx-12B and the 24 patient-derived mouse xenograft tumors that were frozen immediately following removal in liquid nitrogen. Specifically, the cultured cell suspensions were first washed three times with cold phosphate buffer

saline (PBS, purchased from Sigma-Aldrich) in order to remove any culture medium-associated proteins. The cells were then pushed through a 29 gauge insulin syringe to further disrupt their plasma membrane and expose the intracellular proteins. 500 μL of a modified RIPA cell lysis buffer was then added to cell suspensions obtained from a 75 cm^2 flask. For the tumor tissue samples, 5 mL of the same modified RIPA buffer (containing 1% of the protease inhibitor cocktails P8340 purchased from Sigma-Aldrich) was added for every gram of tissue. A tissue grinder was then used for manual disruption of tumor tissue. Once the culture cell suspensions and the ground tumor tissues were sufficiently disrupted, they were centrifuged at 4000*g* for 5 min. The resulting supernatant solutions were further centrifuged at 20000*g* for 20 min in order to fully discard any remaining cell debris. Ten micrograms of proteins from each sample diluted in Laemmli buffer was then heated to 92 °C for 3 to 5 min to allow for sufficient denaturing. They were then loaded onto the wells of a 15% acrylamide gel for proper separation of proteins according molecular weight. Following migration, the proteins were then transferred from the acrylamide gel onto an Amersham Hybond ECL nitrocellulose membrane (GE Healthcare Life Sciences). Each membrane was immersed in appropriate blocking buffer solution (PBS with 0.2% TWEEN 20 with 3% of BSA or 3% of milk) for two hours at room temperature. Incubation with the primary antibodies diluted in PBS with 0.2% TWEEN 20 with 3% of BSA for anti-TSPO antibodies and 3% of milk for the anti α-tubulin antibody, respectively (1/20000 dilution of the anti α-tubulin antibody purchased from Sigma-Aldrich; 1/5000 of the anti-human TSPO antibody Mab 8D7[35,36] generously provided by Dr. E. Bribes of Sanofi-Aventis, France; and 1/10000 dilution of the anti-murine TSPO antibody NP155[37] generously provided by Dr. M. Higuchi, NIRS, Japan), was performed at room temperature for two hours. Following three 10 min wash sessions (under mechanical agitation) with PBS with 0.2% TWEEN 20, the membranes were then incubated with the appropriate secondary antibodies diluted in PBS with 0.2% TWEEN 20 with 1% of BSA or 1% of milk for one hour at room temperature. After three 10 min wash sessions, the membranes were then developed using an Amersham ECL Western Blotting System (GE Healthcare Life Sciences) onto films. For every set of proteins incubated with the anti-human-TSPO antibody, an aliquot of protein extracted from a reference sample of MDA-MB-231 cells was used as a positive control and a MCF-7 cell sample was used as a negative control. All of the human TSPO expression was normalized to that of MDA-MB-231 cells. Conversely, for every set of proteins incubated with the anti-mouse-TSPO antibody, an aliquot of protein extracted a reference sample of PyMT mouse tumor tissue was used as a positive control as well as a normalization factor during analysis. Furthermore, the TSPO content of each protein sample was also normalized by the α-tubulin amount measured in the same sample.

Autoradiography and Competitive Binding Assay. Tumors were excised from mice and fixed in 4% paraformaldehyde (PFA) for 24 h, and then they were treated with 15% sucrose in PBS for 24 h and finally frozen in isopentane in the presence of liquid nitrogen and then kept at −80 °C. The 10 μm thick crysections were then immersed in Tris Buffer (50 mM TRIZMA preset crystals purchased from Sigma-Aldrich) adjusted to pH 7.4 with NaCl containing 74 MBq of [^{18}F]DPA-714 either alone or in the presence of 20 μM unlabeled DPA-714 or PK 11195, for 20 min at room temperature. The unbound excess ligands were removed by two 2 min wash cycles in cold buffer and then a final rinse in cold deionized water. The slides were then quickly dried and exposed to a Kodak Biomax film (purchased from Sigma-Aldrich) overnight.

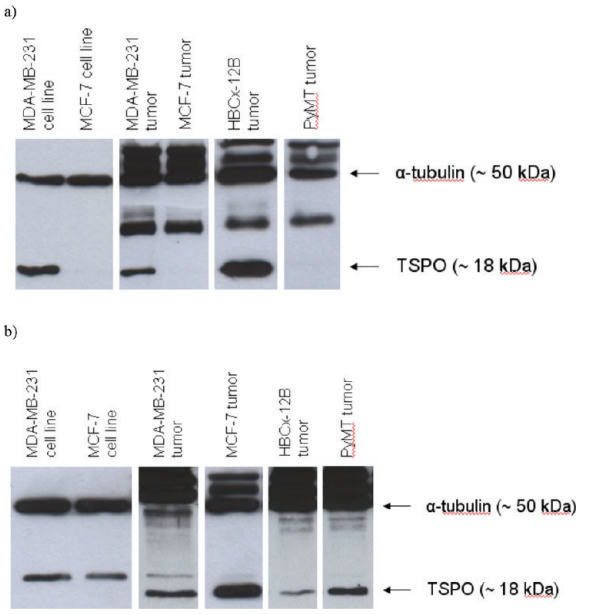

Figure 1. Expression levels of human (a) and murine (b) TSPO measured in proteins extracted from two human cell lines of breast cancer (MDA-MB-231 and MCF-7), and from the tissue of three human xenografts of breast cancer (MDA-MB-231, MCF-7 and HBCx-12B) and the murine PyMT mammary tumor subcutaneously grown in mice.

Immunohistochemistry. The tumor slides were prepared from excised tissues using the same protocol as for autoradiography and then stored at −80 °C. The immunohistochemistry staining protocol has been previously reported by Martin et al.[38] Briefly, the tissue slides were first fixed in 4% PFA for 15 min and then rinsed with PBS. PBS containing NH_4Cl (50 mM in aqueous form) was used to block the PFA for 5 min. After rinsing with PBS, a mixture composed of methanol and acetone (1:1, v:v) was added to the slides for 5 min in order to permeabilize the tissues, and then the slides were left for 5 min in a solution of 0.1% Triton diluted in PBS, and then underwent another PBS wash. The slides were then incubated for 15 min in a blocking solution made up of 5% BSA diluted in PBS containing 0.5% TWEEN 20. The incubation with the primary antibodies (1 μg/mL of the anti-mouse TSPO NP155, 1 μg/mL of the F4/80 pan-macrophage purchased from Abcam, or 1 μg/mL of a rat anti-mouse CD3 antibody purchased from AbD Serotec) occurred at room temperature for 1 h. The excess antibody was removed by three consecutive wash cycles with PBS. Then the appropriate secondary antibodies coupled with fluorophores (goat anti-rat IgG with Alexa Fluor 594 nm for F4/80 or CD3 and goat anti-rabbit IgG with Alexa Fluor 488 nm for the murine anti-TSPO antibody NP155) were added to each slide for 30 min, following by another three washes with PBS. On each slide, a small tissue section was only incubated with the secondary antibody (without the primary antibody) in order to act as controls. Finally, the ProLong gold antifade reagent with 4′,6-diamidino-2-phenylindole (DAPI, purchased from Invitrogen) was used both to stain the cell nuclei and to mount the slide. Fluorescent microscopy was performed using a Zeiss AxioCam with a HXP120 module (Carl Zeiss S.A.S.).

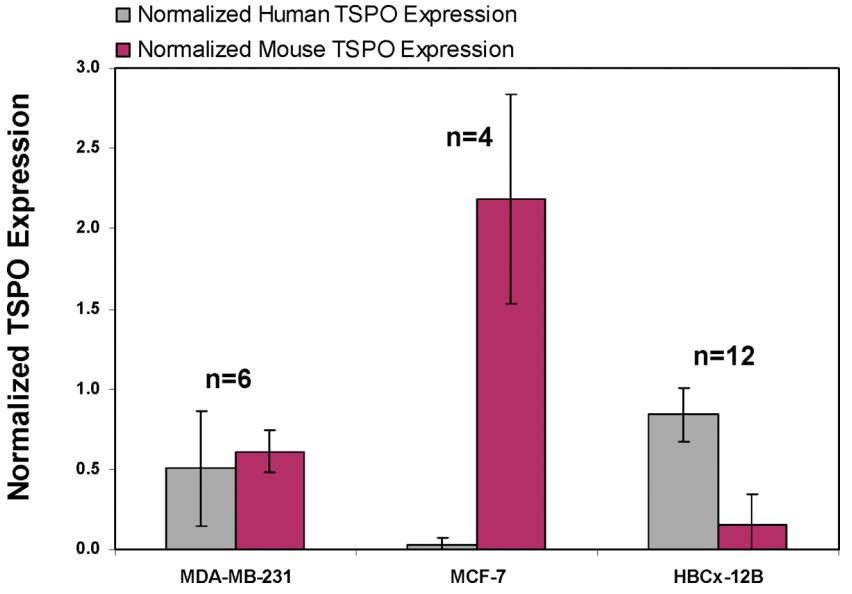

Figure 2. Relative expression levels of the human and mouse TSPO in three human breast cancer xenografts. The normalized human and mouse TSPO expression is the ratio between the human TSPO level measured in each xenograft and that measured from a sample of MDA-MB-231 cultured cells, and the ratio between the mouse TSPO level measured in each xenograft and that measured from a sample of murine PyMT tumor, respectively.

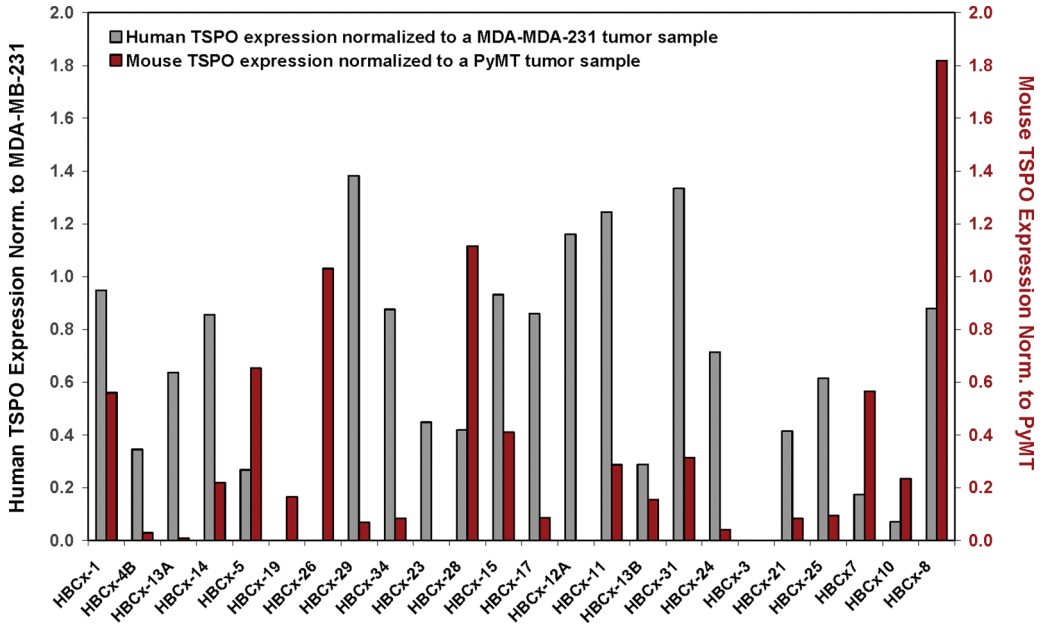

Figure 3. Screening of 24 patient-derived human breast cancer tumors propagated in immunocompromised mice for expression levels of the neoplastic cell-associated TSPO (gray bars) and the tumor stroma-associated TSPO (red bars). Note that HBCx-3 tumor did not have any detectable amount of either form of TSPO.

RESULTS

Assessment of TSPO Expression in Breast Cancer Cell Lines and Tumor Tissues. By employing Western blot with two highly specific anti-TSPO antibodies (one highly specific to the human form of TSPO[35] and one highly specific to the murine form of TSPO[37]), the degree of TSPO expression in the MDA-MB-231 and MCF-7 human breast cancer cell lines was compared, and the results confirmed that TSPO is upregulated in the former but not in the latter (Figure 1a), in accordance with previously reported results.[9] Western blot analysis using the anti-murine TSPO, however, reveals that there is significant expression of TSPO by the tumor stroma cells of murine origin. In particular, the TSPO-negative MCF-7 tumor had a more elevated murine TSPO expression than the TSPO-positive MDA-MB-231 tumor (Figure 1b). The human and murine TSPO expressions were also measured in the HBCx-12B tumor (Figure 2), in addition to the MDA-MB-231 and MCF-7 tumors, and across a panel of 24 other patient-derived human breast cancer xenografts (Figure 3). These results indicate that when tumors of human origin form in immunocompromised mice, the overall tumor TSPO density is contributed by the

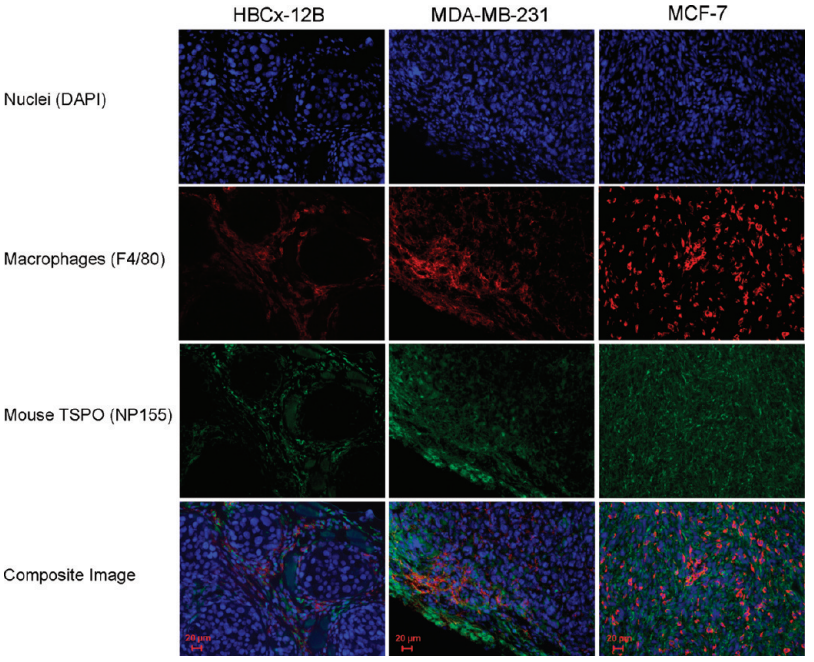

Figure 4. Immunochemical staining of cryopreserved tumor tissue sections obtained from mice bearing the HBCx-12b (left column), MDA-MB-231 (middle column) and MCF-7 (right column) human xenografts. The nuclear stain DAPI is shown in blue, the mouse TSPO in green and the pan-macrophage marker F4/80 in red.

TSPO expression by the human cancer cells as well as by the mouse host cells (i.e., macrophages). It is important to note in Figure 3 that there is a wide range of expression levels of both the cancer cell-associated TSPO and the tumor host cell-associated TSPO across the panel of patient-derived human breast cancer tumors propagated in mice. The expression levels of the human and mouse TSPO did not yield a clear correlation (Appendix, Figure A1).

Marangoni et al.[32] have previously reported some clinical and biological characteristics of 14 of these 24 tumor types. The TSPO levels measured in this study did not directly correlate to the growth rate, metastatic potential or drug responsiveness of these tumors reported by Marangoni et al.[32] (Appendix, Figure A2).

Identification of the Tumor Stroma Cell Type with Expression of TSPO. Immunohistochemical staining of tissue slides obtained from the three different tumor types (MDA-MB-231, MCF-7 and HBCx-12B) was performed with the F4/80 antibody for recognition of the murine macrophages and with the NP155 antibody targeted to murine TSPO. Figure 4 illustrates with representative images obtained from the tissue slides of the three tumor types that, qualitatively, for all three tumor models, the majority of the F4/80 positive cells were also positively stained by the NP155 mouse TSPO antibody. However, there is no physical overlap of the two fluorescent signals because the F4/80 antigen is expressed on the macrophage cell surface, while the TSPO protein is mainly expressed intracellularly, on the mitochondrial membrane.[39,40] Qualitatively, the HBCx-12B tumor (Figure 4) has the lowest macrophage density and murine TSPO expression, the MDA-MB-231 tumor has intermediate macrophage density and murine TSPO expression, and the MCF-7 tumor has the highest macrophage density (infiltrated throughout the tumor tissue) and murine TSPO, all in accordance with the Western blot results (Figure 2). However, it can be noted, in all three cases, that there is some expression of the murine TSPO

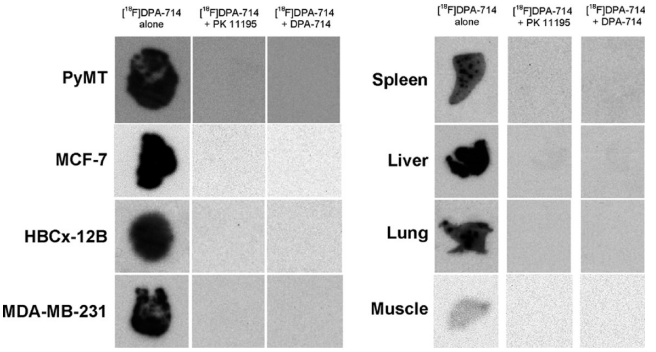

Figure 5. Autoradiography of tumor and healthy tissue cryosections. The left column illustrates the tissue binding characteristics of the TSPO radioligand [^{18}F]DPA-714, while the middle and the right columns show the complete binding inhibition of the radioligand in the presence of 2000-fold excess of non-radiolabeled TSPO ligands DPA-714 and PK 11195, respectively.

in cells that are not F4/80 positive. Previous studies have reported that other inflammatory cells such as T cells,[41] monocytes[42,43] and neutrophils[42,44] can also express TSPO. For example, in a representative MCF-7 tumor tissue section (Appendix, Figure A3), some TSPO expression (green) can be seen in T-cells that are positively stained for CD3 (red).

[^{18}F]DPA-714 Binding to Human and Murine TPSO. To further support the claim that TSPO expressed by mouse host cells plays a significant role in the overall tumor TSPO density, *ex vivo* autoradiography was conducted using the radioligand [^{18}F]DPA-714 on cryosections of tumor and normal tissues collected from tumor-bearing mice, in both the absence and presence of excess non-radiolabeled TSPO ligands DPA-714 and PK 11195. Figure 5 illustrates that, in all tissues, the binding of

[^{18}F]DPA-714 is specific, because when coincubated with a 2000-fold excess of nonlabeled ligands, no significant radioactive signal (above background) is detected after washing. This implies that the majority of the TSPO binding sites were occupied by the competing non-radiolabeled compounds DPA-714 and PK 11195. Partial binding inhibition of the radioligand was achieved with the incubation of a 100-fold excess of the non-radiolabeled TSPO ligand DPA-714 (Appendix, Figure A4). From Figure 5, it is reasonable to conclude that the four tumor tissues (murine tumor PyMT and human xenografts MDA-MB-231, MCF-7 and HBCx-12B) have substantially higher [^{18}F]DPA-714 binding than healthy muscle, which was used as the negative control, because it is known to have no TSPO expression. It is important to note that the MCF-7 tumor, although it has very little inherent expression of TSPO by the MCF-7 cancer cells (Figures 1 and 2), yields a very strong signal when incubated with the TSPO ligand [^{18}F]DPA-714, due to the presence of stromal cell-associated TSPO (Figures 2, 4 and A3). In the spleen and lung tissue sections, it can be observed that the [^{18}F]DPA-714 binding is nonhomogeneous; the morphology of the spatial localization of [^{18}F]DPA-714 in these two organs may suggest that the ligands are actually bound to targets found within the circulating bloodstream, as the [^{18}F]DPA-714 distribution looks to be confined within blood vessel-like structures. Finally, the liver was the positive control, as it has been previously shown to highly accumulate TSPO ligands *in vivo*.[45,46]

DISCUSSION

The role of TSPO has been much investigated in the central nervous system (CNS)[25,47,48] and a number of positron emission tomography (PET) tracers[49] (i.e., [^{11}C]PK 11195, [^{11}C]DAA1106 and [^{11}C]PBR28) have been successfully developed to characterize this receptor in patients with a range of diseases (i.e., Alzheimer's, multiple sclerosis and ischemic stroke). The potential of employing TSPO ligands as neuroimaging biomakers is still under evaluation. More recently, there has been growing interest in assessing different TSPO ligands for therapeutic applications.[50−55]

In the periphery, the potential use of TSPO ligands for both imaging and therapy is gaining increasing attention. To date, researchers have explored the role of TSPO in atherosclerosis,[11,56,57] arthritis[12,58,59] and cancer.[8,60,61] In atherosclerosis and arthritis, TSPO ligands have been employed to monitor the activity of the immune system, such as macrophage burden.[56] In cancer, however, there are multiple cell types (i.e., breast, colorectal, prostate, ovarian, glioma and hepatocarcinoma) that have been found to overexpress TSPO.[8,62] In breast cancer, much of the work thus far has been concentrated in identifying which cancer cell types overexpress TSPO[9,63−69] and whether this overexpression could be used to correlate with disease burden and clinical outcome.[10] This work demonstrates, for the first time, that the overall TSPO expression in a tumor, which has the potential to be used as prognostic factor for predicting clinical outcome,[10,62,70] is contributed by both its neoplastic and stromal components. As a result, it has implications on how the TSPO expression level in a tumor should be evaluated both histologically and using imaging and therapeutic ligands. It is interesting to note that although studies in breast cell lines have demonstrated that TSPO overexpression can be correlated to aggressive phenotype,[9] the clinical study reported by Galiegue et al.[10] found that TSPO expression did not affect disease-free survival in the whole population but it positively correlated with a shorter disease-free survival in the lymph node negative patients. In light of the findings reported here, independent characterization of the neoplastic cell-associated TSPO expression and the inflammatory cell-associated TSPO expression would perhaps lead to a more pronounced clinical significance. For example, the degree of inflammation in breast cancer has been reported to correlate to angiogenesis, metastatic potential[17,22] and poor prognosis in patients.[20] The overexpression of TSPO in both the neoplastic and the stromal components of a tumor could also be a result of mutual interaction and cross-talk between the cancer cells and their microenvironment, a process that is similar to that of chemokine production (i.e., CXCL12).[71] Therefore, successful unmixing of the TSPO overexpression in the different cell populations that make up the tumor may further enhance the prognostic value of this protein and potentially provide an additional parameter for biological characterization of cancer signatures.

The preliminary screening of the neoplastic and stromal TSPO expressions in the panel of 25 patient-derived breast tumors (including the HBCx-12B) propagated in mice has confirmed that the majority of these (80%, 20 out of 25) had either (1) a human (neoplastic) TSPO expression level equal to or greater than 40% of the receptor density measured in a MDA-MB-231 tumor, a tumor cell type often used as a reference for high TSPO expression,[9,66−68] or (2) a murine (stromal) TSPO expression level equal to or greater than 40% of that of a reference high TSPO expressing murine PyMT tumor. These results are in accordance with the clinical study reported by Galiegue et al.[10] in which 80% (94 out of 117) of the patient breast tumor tissues exhibited strong (scores 2 or 3) TSPO immunostaining. This dominant trend of TSPO expression by breast cancers suggests that this protein may play an important role in tumor progression and potentially response to therapy.

The successful employment of an established TSPO ligand DPA-714[33,72] in this investigation for assessment of the overall tumor tissue TSPO expression demonstrates that existing TSPO ligands developed for imaging and treatment of CNS disease can be translated for use in oncology applications in the periphery. However, in light of this new evidence that different cell types within the tumor contribute to its overall TSPO expression level, further research should be directed toward the development of *ex vivo* and *in vivo* assays with the capability to quantify the relative contributions of the neoplastic and the stromal components. The ability to discriminate the neoplastic and stromal TSPO expressions in a tumor has the potential of providing a powerful toolset for improved diagnosis, staging, prognosis assessment and treatment follow-up of breast cancers.

ABBREVIATIONS USED

TSPO, translocator protein; PBR, peripheral benzodiazepine receptor; DPA-714, *N*,*N*-diethyl-2-(2-(4-(2-fluoroethoxy)phenyl)-5,7-dimethylpyrazolo[1,5-*a*]pyrimidin-3-yl)acetamide; PyMT, Polyoma Middle T oncoprotein; TAMs, tumor-associated macrophages; MMTV, mouse mammary tumor virus; SAA, serum amyloid A; DMEM, Dulbecco's modified Eagle's medium; FBS, fetal bovine serum; PBS, phosphate buffer saline; PFA, paraformaldehyde; DAPI, 4′,6-diamidino-2-phenylindole; PET, positron emission tomography; EMIL, European Molecular Imaging Laboratories; ARC, Association pour la Recherche sur le Cancer

APPENDIX

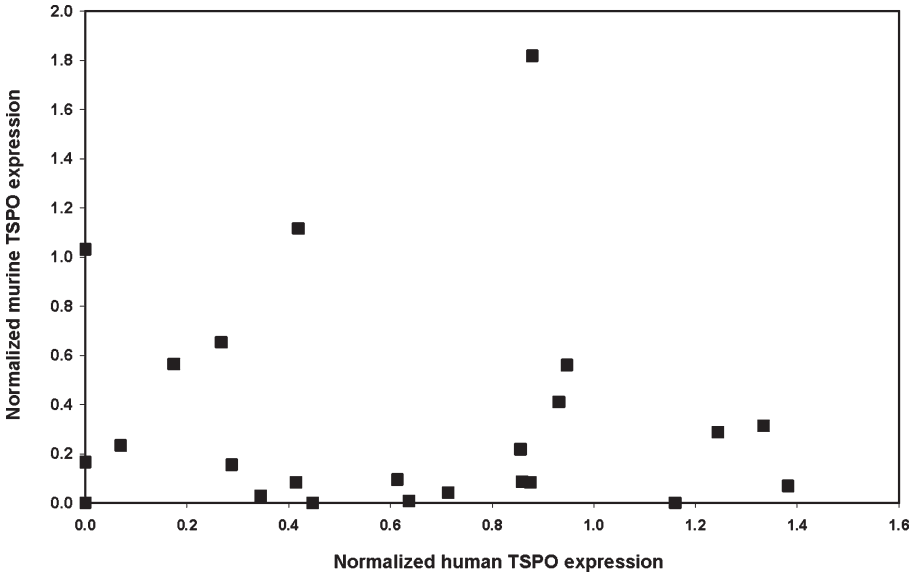

Figure A1. Screening of 24 patient-derived human breast cancer tumors propagated in immunocompromised mice did not yield a clear correlation between the neoplastic (human) cell-associated TSPO and the tumor stroma-associated TSPO expression levels.

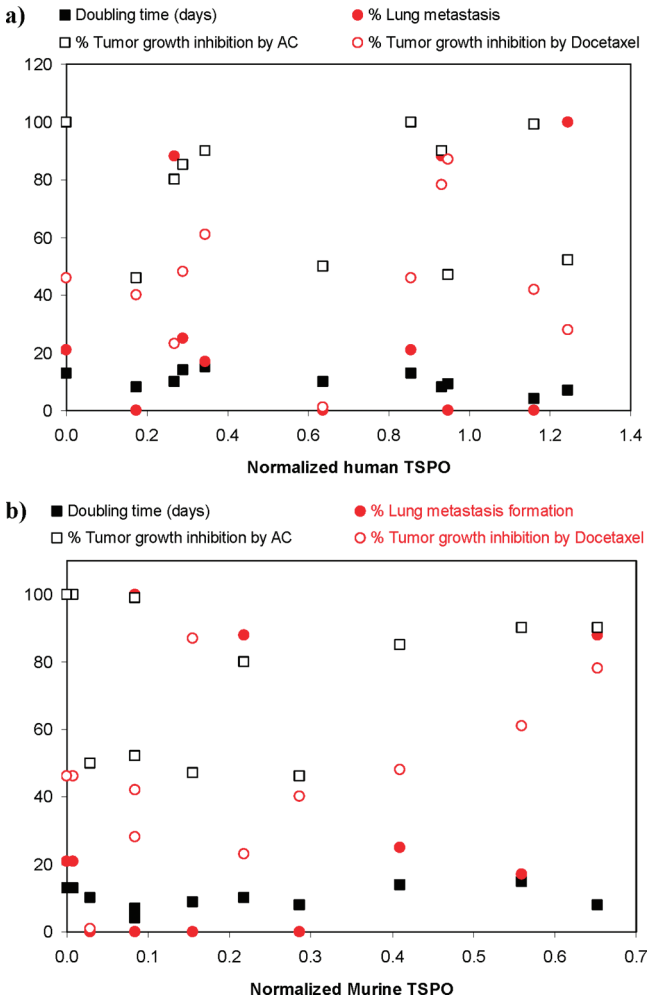

Figure A2. (a) Neoplastic cell-associated and (b) host murine stroma-associated TSPO expression levels vs xenograft doubling time in days (filled black squares), % lung metastasis formation (filled red circles), % tumor growth inhibition following treatment with an adriamycin-cyclophosphamide combination (AC, hollow black squares), and % tumor growth inhibition following treatment with docetaxel (hollow red circles).

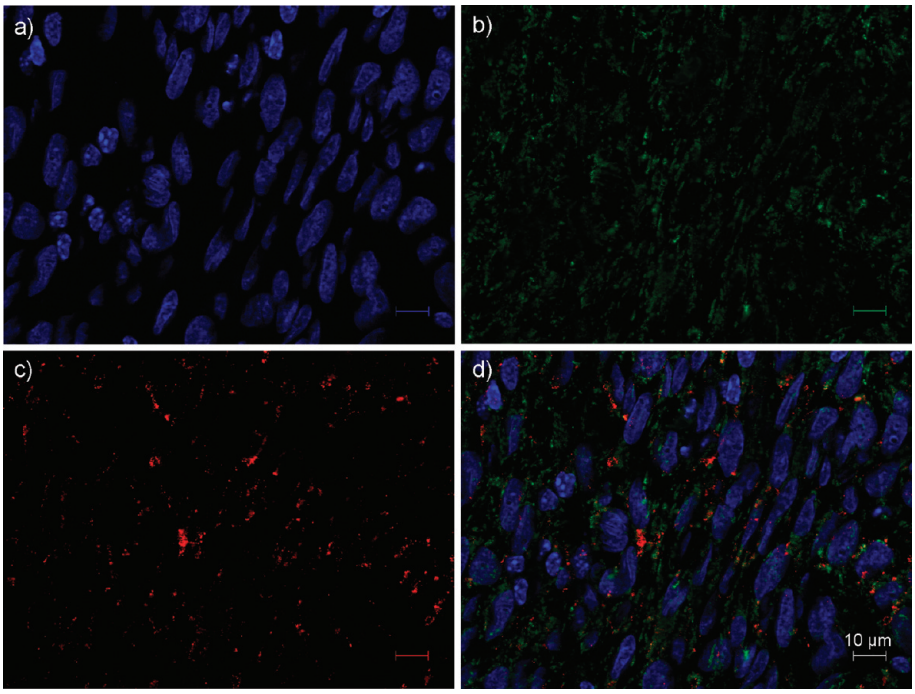

Figure A3. A representative tissue section from a MCF-7 tumor costained with (a) DAPI for nuclei, (b) NP155 for murine TSPO, and (c) CD3 for mature murine T-cells. The lower right quadrant (d) is a composite image illustrating the presence of cells which are positively stained for both NP155 and CD3, and others which are only positively stained with NP155 alone.

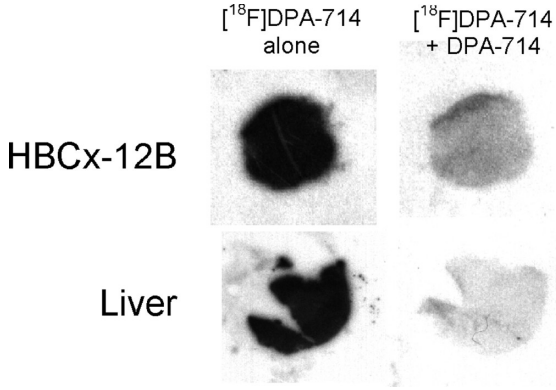

Figure A4. Autoradiography of representative tumor and liver cryosections incubated with the radioligand [^{18}F]DPA-714 alone (left column) and with the addition of a low amount (100-fold) of non-radiolabeled DPA-714 (right column). Partial inhibition of binding of the radioligand was achieved.

AUTHOR INFORMATION

Corresponding Author

*Laboratoire d'Imagerie Moléculaire Expérimentale, INSERM Unit 1023, CEA-DSV-I^{2}BM, Service Hospitalier Frédéric Joliot, 4 Place du Général Leclerc, 91400 Orsay Cedex, France. Phone: + 33 1 69 86 77 79. Fax: +33 1 69 86 77 68. E-mail: bertrand.tavitian@cea.fr.

ACKNOWLEDGMENT

Funding from Cancéropôle Île-de-France and the European Molecular Imaging Laboratories (EMIL) supported this work. J. Zheng is grateful for the Association pour la Recherche sur le Cancer (ARC) Young Researcher Postdoctoral Fellowship. The authors would also like to thank B. Thézé for his expertise and help with the immunohistochemistry experiments, A. Winkeler for fruitful scientific discussions, and Dr. E. Bribes and Dr. M. Higuchi for generously providing the antibodies Mab 8D7 and NP155, repectively.

REFERENCES

(1) *Cancer Statistics 2009 Presentation*; American Cancer Society: 2009.
(2) Gonda, T. A.; Tu, S.; Wang, T. C. Chronic inflammation, the tumor microenvironment and carcinogenesis. *Cell Cycle* **2009**, *8* (13), 2005–13.
(3) Hanahan, D.; Weinberg, R. A. The hallmarks of cancer. *Cell* **2000**, *100* (1), 57–70.
(4) Joyce, J. A.; Pollard, J. W. Microenvironmental regulation of metastasis. *Nat. Rev. Cancer* **2009**, *9* (4), 239–52.
(5) Lorusso, G.; Ruegg, C. The tumor microenvironment and its contribution to tumor evolution toward metastasis. *Histochem. Cell Biol.* **2008**, *130* (6), 1091–103.
(6) Mantovani, A.; Romero, P.; Palucka, A. K.; Marincola, F. M. Tumour immunity: effector response to tumour and role of the microenvironment. *Lancet* **2008**, *371* (9614), 771–83.
(7) Siveen, K. S.; Kuttan, G. Role of macrophages in tumour progression. *Immunol. Lett.* **2009**, *123* (2), 97–102.
(8) Corsi, L.; Geminiani, E.; Baraldi, M. Peripheral benzodiazepine receptor (PBR) new insight in cell proliferation and cell differentiation review. *Curr. Clin. Pharmacol.* **2008**, *3* (1), 38–45.
(9) Hardwick, M.; Fertikh, D.; Culty, M.; Li, H.; Vidic, B.; Papadopoulos, V. Peripheral-type benzodiazepine receptor (PBR) in human breast cancer: correlation of breast cancer cell aggressive phenotype with PBR expression, nuclear localization, and PBR-mediated cell proliferation and nuclear transport of cholesterol. *Cancer Res.* **1999**, *59* (4), 831–42.
(10) Galiegue, S.; Casellas, P.; Kramar, A.; Tinel, N.; Simony-Lafontaine, J. Immunohistochemical assessment of the peripheral benzodiazepine receptor in breast cancer and its relationship with survival. *Clin. Cancer Res.* **2004**, *10* (6), 2058–64.

(11) Fujimura, Y.; Hwang, P. M.; Trout Iii, H.; Kozloff, L.; Imaizumi, M.; Innis, R. B.; Fujita, M. Increased peripheral benzodiazepine receptors in arterial plaque of patients with atherosclerosis: An autoradiographic study with [(3)H]PK 11195. *Atherosclerosis* **2008**, *201* (1), 108–11.

(12) van der Laken, C. J.; Elzinga, E. H.; Kropholler, M. A.; Molthoff, C. F.; van der Heijden, J. W.; Maruyama, K.; Boellaard, R.; Dijkmans, B. A.; Lammertsma, A. A.; Voskuyl, A. E. Noninvasive imaging of macrophages in rheumatoid synovitis using 11C-(R)-PK11195 and positron emission tomography. *Arthritis Rheum.* **2008**, *58* (11), 3350–5.

(13) Venneti, S.; Lopresti, B. J.; Wiley, C. A. The peripheral benzodiazepine receptor (Translocator protein 18 kDa) in microglia: from pathology to imaging. *Prog. Neurobiol.* **2006**, *80* (6), 308–22.

(14) Chauveau, F.; Boutin, H.; Van Camp, N.; Dolle, F.; Tavitian, B. Nuclear imaging of neuroinflammation: a comprehensive review of [11C]PK11195 challengers. *Eur. J. Nucl. Med. Mol. Imaging* **2008**, *35* (12), 2304–19.

(15) Doorduin, J.; de Vries, E. F.; Dierckx, R. A.; Klein, H. C. PET imaging of the peripheral benzodiazepine receptor: monitoring disease progression and therapy response in neurodegenerative disorders. *Curr. Pharm. Des.* **2008**, *14* (31), 3297–315.

(16) Colotta, F.; Allavena, P.; Sica, A.; Garlanda, C.; Mantovani, A. Cancer-related inflammation, the seventh hallmark of cancer: links to genetic instability. *Carcinogenesis* **2009**, *30* (7), 1073–81.

(17) DeNardo, D. G.; Barreto, J. B.; Andreu, P.; Vasquez, L.; Tawfik, D.; Kolhatkar, N.; Coussens, L. M. CD4(+) T cells regulate pulmonary metastasis of mammary carcinomas by enhancing protumor properties of macrophages. *Cancer Cell* **2009**, *16* (2), 91–102.

(18) Lin, E. Y.; Li, J. F.; Bricard, G.; Wang, W.; Deng, Y.; Sellers, R.; Porcelli, S. A.; Pollard, J. W. Vascular endothelial growth factor restores delayed tumor progression in tumors depleted of macrophages. *Mol. Oncol.* **2007**, *1* (3), 288–302.

(19) Ono, M. Molecular links between tumor angiogenesis and inflammation: inflammatory stimuli of macrophages and cancer cells as targets for therapeutic strategy. *Cancer Sci.* **2008**, *99* (8), 1501–6.

(20) Pierce, B. L.; Ballard-Barbash, R.; Bernstein, L.; Baumgartner, R. N.; Neuhouser, M. L.; Wener, M. H.; Baumgartner, K. B.; Gilliland, F. D.; Sorensen, B. E.; McTiernan, A.; Ulrich, C. M. Elevated biomarkers of inflammation are associated with reduced survival among breast cancer patients. *J. Clin. Oncol.* **2009**, *27* (21), 3437–44.

(21) Folkman, J. Tumor angiogenesis. *Adv. Cancer Res.* **1985**, *43* 175–203.

(22) Lin, E. Y.; Li, J. F.; Gnatovskiy, L.; Deng, Y.; Zhu, L.; Grzesik, D. A.; Qian, H.; Xue, X. N.; Pollard, J. W. Macrophages regulate the angiogenic switch in a mouse model of breast cancer. *Cancer Res.* **2006**, *66* (23), 11238–46.

(23) Huysentruyt, L. C.; Seyfried, T. N. Perspectives on the mesenchymal origin of metastatic cancer. *Cancer Metastasis Rev.* **2010**, *29* (4), 695–707.

(24) Rupprecht, R.; Papadopoulos, V.; Rammes, G.; Baghai, T. C.; Fan, J.; Akula, N.; Groyer, G.; Adams, D.; Schumacher, M. Translocator protein (18 kDa) (TSPO) as a therapeutic target for neurological and psychiatric disorders. *Nat. Rev. Drug Discovery* **2010**, *9* (12), 971–88.

(25) Chen, M. K.; Guilarte, T. R. Translocator protein 18 kDa (TSPO): molecular sensor of brain injury and repair. *Pharmacol. Ther.* **2008**, *118* (1), 1–17.

(26) Guo, P.; Ma, J.; Li, S.; Guo, Z.; Adams, A. L.; Gallo, J. M. Targeted delivery of a peripheral benzodiazepine receptor ligand-gemcitabine conjugate to brain tumors in a xenograft model. *Cancer Chemother. Pharmacol.* **2001**, *48* (2), 169–76.

(27) Laquintana, V.; Denora, N.; Musacchio, T.; Lasorsa, M.; Latrofa, A.; Trapani, G. Peripheral benzodiazepine receptor ligand-PLGA polymer conjugates potentially useful as delivery systems of apoptotic agents. *J. Controlled Release* **2009**, *137* (3), 185–95.

(28) Manning, H. C.; Goebel, T.; Thompson, R. C.; Price, R. R.; Lee, H.; Bornhop, D. J. Targeted molecular imaging agents for cellular-scale bimodal imaging. *Bioconjugate Chem.* **2004**, *15* (6), 1488–95.

(29) Musacchio, T.; Laquintana, V.; Latrofa, A.; Trapani, G.; Torchilin, V. P. PEG-PE micelles loaded with paclitaxel and surface-modified by a PBR-ligand: synergistic anticancer effect. *Mol. Pharmaceutics* **2009**, *6* (2), 468–79.

(30) Samuelson, L. E.; Dukes, M. J.; Hunt, C. R.; Casey, J. D.; Bornhop, D. J. TSPO targeted dendrimer imaging agent: synthesis, characterization, and cellular internalization. *Bioconjugate Chem.* **2009**, *20* (11), 2082–9.

(31) Trapani, G.; Laquintana, V.; Latrofa, A.; Ma, J.; Reed, K.; Serra, M.; Biggio, G.; Liso, G.; Gallo, J. M. Peripheral benzodiazepine receptor ligand-melphalan conjugates for potential selective drug delivery to brain tumors. *Bioconjugate Chem.* **2003**, *14* (4), 830–9.

(32) Marangoni, E.; Vincent-Salomon, A.; Auger, N.; Degeorges, A.; Assayag, F.; de Cremoux, P.; de Plater, L.; Guyader, C.; De Pinieux, G.; Judde, J. G.; Rebucci, M.; Tran-Perennou, C.; Sastre-Garau, X.; Sigal-Zafrani, B.; Delattre, O.; Dieras, V.; Poupon, M. F. A new model of patient tumor-derived breast cancer xenografts for preclinical assays. *Clin. Cancer Res.* **2007**, *13* (13), 3989–98.

(33) James, M. L.; Fulton, R. R.; Vercoullie, J.; Henderson, D. J.; Garreau, L.; Chalon, S.; Dolle, F.; Costa, B.; Guilloteau, D.; Kassiou, M. DPA-714, a new translocator protein-specific ligand: synthesis, radiofluorination, and pharmacologic characterization. *J. Nucl. Med.* **2008**, *49* (5), 814–22.

(34) Damont, A.; Hinnen, F.; Kuhnast, B.; Schöllhorn-Peyronneau, M.-A.; James, M. L.; Luus, C.; Tavitian, B.; Kassiou, M.; Dollé, F. Radiosynthesis of [^{18}F]DPA-714, a selective radioligand for imaging the translocator protein (18 kDa) with PET. *J. Labelled Compd. Radiopharm.* **2008**, *51* (7−8), 286–292.

(35) Bribes, E.; Carriere, D.; Goubet, C.; Galiegue, S.; Casellas, P.; Simony-Lafontaine, J. Immunohistochemical assessment of the peripheral benzodiazepine receptor in human tissues. *J. Histochem. Cytochem.* **2004**, *52* (1), 19–28.

(36) Dussossoy, D.; Carayon, P.; Feraut, D.; Belugou, S.; Combes, T.; Canat, X.; Vidal, H.; Casellas, P. Development of a monoclonal antibody to immuno-cytochemical analysis of the cellular localization of the peripheral benzodiazepine receptor. *Cytometry* **1996**, *24* (1), 39–48.

(37) Ji, B.; Maeda, J.; Sawada, M.; Ono, M.; Okauchi, T.; Inaji, M.; Zhang, M. R.; Suzuki, K.; Ando, K.; Staufenbiel, M.; Trojanowski, J. Q.; Lee, V. M.; Higuchi, M.; Suhara, T. Imaging of peripheral benzodiazepine receptor expression as biomarkers of detrimental versus beneficial glial responses in mouse models of Alzheimer's and other CNS pathologies. *J. Neurosci.* **2008**, *28* (47), 12255–67.

(38) Martin, A.; Boisgard, R.; Theze, B.; Van Camp, N.; Kuhnast, B.; Damont, A.; Kassiou, M.; Dolle, F.; Tavitian, B. Evaluation of the PBR/TSPO radioligand [(18)F]DPA-714 in a rat model of focal cerebral ischemia. *J. Cereb. Blood Flow Metab.* **2010**, *30* (1), 230–41.

(39) Anholt, R. R.; Pedersen, P. L.; De Souza, E. B.; Snyder, S. H. The peripheral-type benzodiazepine receptor. Localization to the mitochondrial outer membrane. *J. Biol. Chem.* **1986**, *261* (2), 576–83.

(40) Culty, M.; Li, H.; Boujrad, N.; Amri, H.; Vidic, B.; Bernassau, J. M.; Reversat, J. L.; Papadopoulos, V. In vitro studies on the role of the peripheral-type benzodiazepine receptor in steroidogenesis. *J. Steroid Biochem. Mol. Biol.* **1999**, *69* (1−6), 123–30.

(41) Miltyk, W.; Pallka, M.; Karna, E.; Jarzabek, K.; Boujrad, N.; Knapp, P. Antimitotic activity of high affinity ligands for peripheral benzodiazepine receptor (PBR) in some normal and neoplastic cell lines. *Adv. Med. Sci.* **2006**, *51*, 156–9.

(42) Canat, X.; Carayon, P.; Bouaboula, M.; Cahard, D.; Shire, D.; Roque, C.; Le Fur, G.; Casellas, P. Distribution profile and properties of peripheral-type benzodiazepine receptors on human hemopoietic cells. *Life Sci.* **1993**, *52* (1), 107–18.

(43) Hardwick, M. J.; Chen, M. K.; Baidoo, K.; Pomper, M. G.; Guilarte, T. R. In vivo imaging of peripheral benzodiazepine receptors in mouse lungs: a biomarker of inflammation. *Mol. Imaging* **2005**, *4* (4), 432–8.

(44) Muhling, J.; Gonter, J.; Nickolaus, K. A.; Matejec, R.; Welters, I. D.; Wolff, M.; Sablotzki, A.; Engel, J.; Krull, M.; Menges, T.; Fuchs, M.; Dehne, M. G.; Hempelmann, G. Benzodiazepine receptor-dependent modulation of neutrophil (PMN) free amino- and alpha-keto acid profiles or immune functions. *Amino Acids* **2005**, *28* (1), 85–98.

(45) Kumar, A.; Muzik, O.; Chugani, D.; Chakraborty, P.; Chugani, H. T. PET-derived biodistribution and dosimetry of the benzodiazepine receptor-binding radioligand (11)C-(R)-PK11195 in children and adults. *J. Nucl. Med.* **2010**, *51* (1), 139–44.

(46) Schweitzer, P. J.; Fallon, B. A.; Mann, J. J.; Kumar, J. S. PET tracers for the peripheral benzodiazepine receptor and uses thereof. *Drug Discovery Today* **2010**, *15* (21−22), 933–42.

(47) Scarf, A. M.; Ittner, L. M.; Kassiou, M. The translocator protein (18 kDa): central nervous system disease and drug design. *J. Med. Chem.* **2009**, *52* (3), 581–92.

(48) Winkeler, A.; Boisgard, R.; Martin, A.; Tavitian, B. Radioisotopic imaging of neuroinflammation. *J. Nucl. Med.* **2010**, *51* (1), 1–4.

(49) Dolle, F.; Luus, C.; Reynolds, A.; Kassiou, M. Radiolabelled molecules for imaging the translocator protein (18 kDa) using positron emission tomography. *Curr. Med. Chem.* **2009**, *16* (22), 2899–923.

(50) Fafalios, A.; Akhavan, A.; Parwani, A. V.; Bies, R. R.; McHugh, K. J.; Pflug, B. R. Translocator protein blockade reduces prostate tumor growth. *Clin. Cancer Res.* **2009**, *15* (19), 6177–84.

(51) Giatti, S.; Pesaresi, M.; Cavaletti, G.; Bianchi, R.; Carozzi, V.; Lombardi, R.; Maschi, O.; Lauria, G.; Garcia-Segura, L. M.; Caruso, D.; Melcangi, R. C. Neuroprotective effects of a ligand of translocator protein-18 kDa (Ro5−4864) in experimental diabetic neuropathy. *Neuroscience* **2009**, *164* (2), 520–9.

(52) Papadopoulos, V.; Lecanu, L. Translocator protein (18 kDa) TSPO: an emerging therapeutic target in neurotrauma. *Exp. Neurol.* **2009**, *219* (1), 53–7.

(53) Sakai, M.; Ferraz-de-Paula, V.; Pinheiro, M. L.; Ribeiro, A.; Quinteiro-Filho, W. M.; Rone, M. B.; Martinez-Arguelles, D. B.; Dagli, M. L.; Papadopoulos, V.; Palermo-Neto, J. Translocator protein (18 kDa) mediates the pro-growth effects of diazepam on Ehrlich tumor cells in vivo. *Eur. J. Pharmacol.* **2010**, *626* (2−3), 131–8.

(54) Soustiel, J. F.; Zaaroor, M.; Vlodavsky, E.; Veenman, L.; Weizman, A.; Gavish, M. Neuroprotective effect of Ro5−4864 following brain injury. *Exp. Neurol.* **2008**, *214* (2), 201–8.

(55) Taliani, S.; Da Settimo, F.; Da Pozzo, E.; Chelli, B.; Martini, C. Translocator protein ligands as promising therapeutic tools for anxiety disorders. *Curr. Med. Chem.* **2009**, *16* (26), 3359–80.

(56) Bird, J. L.; Izquierdo-Garcia, D.; Davies, J. R.; Rudd, J. H.; Probst, K. C.; Figg, N.; Clark, J. C.; Weissberg, P. L.; Davenport, A. P.; Warburton, E. A. Evaluation of translocator protein quantification as a tool for characterising macrophage burden in human carotid atherosclerosis. *Atherosclerosis* **2010**, *210* (2), 388–91.

(57) Dimitrova-Shumkovska, J.; Veenman, L.; Ristoski, T.; Leschiner, S.; Gavish, M. Chronic high fat, high cholesterol supplementation decreases 18 kDa Translocator Protein binding capacity in association with increased oxidative stress in rat liver and aorta. *Food Chem. Toxicol.* **2010**, *48* (3), 910–21.

(58) Bazzichi, L.; Betti, L.; Giannaccini, G.; Rossi, A.; Lucacchini, A. Peripheral-type benzodiazepine receptors in human mononuclear cells of patients affected by osteoarthritis, rheumatoid arthritis or psoriasic arthritis. *Clin. Biochem.* **2003**, *36* (1), 57–60.

(59) Bressan, E.; Farges, R. C.; Ferrara, P.; Tonussi, C. R. Comparison of two PBR ligands with classical antiinflammatory drugs in LPS-induced arthritis in rats. *Life Sci.* **2003**, *72* (23), 2591–601.

(60) Decaudin, D. Peripheral benzodiazepine receptor and its clinical targeting. *Anticancer Drugs* **2004**, *15* (8), 737–45.

(61) Papadopoulos, V. Peripheral benzodiazepine receptor: structure and function in health and disease. *Ann. Pharm. Fr.* **2003**, *61* (1), 30–50.

(62) Han, Z.; Slack, R. S.; Li, W.; Papadopoulos, V. Expression of peripheral benzodiazepine receptor (PBR) in human tumors: relationship to breast, colorectal, and prostate tumor progression. *J. Recept. Signal Transduction Res.* **2003**, *23* (2−3), 225–38.

(63) Beinlich, A.; Strohmeier, R.; Kaufmann, M.; Kuhl, H. Specific binding of benzodiazepines to human breast cancer cell lines. *Life Sci.* **1999**, *65* (20), 2099–108.

(64) Beinlich, A.; Strohmeier, R.; Kaufmann, M.; Kuhl, H. Relation of cell proliferation to expression of peripheral benzodiazepine receptors in human breast cancer cell lines. *Biochem. Pharmacol.* **2000**, *60* (3), 397–402.

(65) Carmel, I.; Fares, F. A.; Leschiner, S.; Scherubl, H.; Weisinger, G.; Gavish, M. Peripheral-type benzodiazepine receptors in the regulation of proliferation of MCF-7 human breast carcinoma cell line. *Biochem. Pharmacol.* **1999**, *58* (2), 273–8.

(66) Hardwick, M.; Cavalli, L. R.; Barlow, K. D.; Haddad, B. R.; Papadopoulos, V. Peripheral-type benzodiazepine receptor (PBR) gene amplification in MDA-MB-231 aggressive breast cancer cells. *Cancer Genet. Cytogenet.* **2002**, *139* (1), 48–51.

(67) Hardwick, M.; Rone, J.; Han, Z.; Haddad, B.; Papadopoulos, V. Peripheral-type benzodiazepine receptor levels correlate with the ability of human breast cancer MDA-MB-231 cell line to grow in SCID mice. *Int. J. Cancer* **2001**, *94* (3), 322–7.

(68) Li, W.; Hardwick, M. J.; Rosenthal, D.; Culty, M.; Papadopoulos, V. Peripheral-type benzodiazepine receptor overexpression and knockdown in human breast cancer cells indicate its prominent role in tumor cell proliferation. *Biochem. Pharmacol.* **2007**, *73* (4), 491–503.

(69) Sanger, N.; Strohmeier, R.; Kaufmann, M.; Kuhl, H. Cell cycle-related expression and ligand binding of peripheral benzodiazepine receptor in human breast cancer cell lines. *Eur. J. Cancer* **2000**, *36* (16), 2157–63.

(70) Maaser, K.; Grabowski, P.; Sutter, A. P.; Hopfner, M.; Foss, H. D.; Stein, H.; Berger, G.; Gavish, M.; Zeitz, M.; Scherubl, H. Overexpression of the peripheral benzodiazepine receptor is a relevant prognostic factor in stage III colorectal cancer. *Clin. Cancer Res.* **2002**, *8* (10), 3205–9.

(71) Raman, D.; Baugher, P. J.; Thu, Y. M.; Richmond, A. Role of chemokines in tumor growth. *Cancer Lett.* **2007**, *256* (2), 137–65.

(72) Chauveau, F.; Van Camp, N.; Dolle, F.; Kuhnast, B.; Hinnen, F.; Damont, A.; Boutin, H.; James, M.; Kassiou, M.; Tavitian, B. Comparative evaluation of the translocator protein radioligands 11C-DPA-713, 18F-DPA-714, and 11C-PK11195 in a rat model of acute neuroinflammation. *J. Nucl. Med.* **2009**, *50* (3), 468–76.